# A Centralized Reactive Power Compensation System for LV Distribution Networks

S. X. Chen, *Member, IEEE*, Y. S. Foo. Eddy, *Student Member, IEEE*, H. B. Gooi, *Senior Member, IEEE*, M. Q. Wang, *Member, IEEE*, and S. F. Lu

***Abstract*—A centralized reactive power compensation system is proposed for low voltage (LV) distribution networks. It can be connected with any bus which needs reactive power. The current industry practice is to locally install reactive power compensation system to maintain the local bus voltage and power factor. By centralizing capacitor banks together, it can help to maintain bus voltages and power factors as well as reduce the power cable losses. Besides, the centralized reactive power system can be easily expanded to meet any future load increase. A reasonably sized centralized reactive power compensation system will be capable of meeting the requirements of the network and the optimization algorithm proposed in this paper can help to find this optimal size by minimizing the expected total cost ($ETCH$). Different load situations and their respective probabilities are also considered in the proposed algorithm. The concept of the centralized reactive power compensation system is applied to a local shipyard power system to verify its effectiveness. The results show that an optimally sized centralized reactive power system exists and is capable of maintaining bus voltages as well as reducing the power losses in the distribution network. A significant power loss reduction can be obtained at the optimal capacity of the centralized reactive power compensation system in the case study.**

***Index Terms*—Capacitors, power distribution planning, reactive power control.**

## NOMENCLATURE

| | |
|---|---|
| $(*)^C$ | $(*)$ injected by centralized capacitor bank. |
| $(*)^D$ | $(*)$ consumed by load bus. |
| $(*)^G$ | $(*)$ from conventional or renewable energy. |
| $(*)^H$ | $(*)$ for high load situation. |
| $(*)^L$ | $(*)$ for low load situation. |
| $(*)^l$ | $(*)$ of distribution line $l$. |
| $(*)^s$ | $(*)$ under load scenario $s$. |
| $(*)^{\max}$ | Maximum value of $(*)$. |
| $(*)^{\min}$ | Minimum value of $(*)$. |
| $(*)_f$ | $(*)$ at $from$ end, $*$ can be voltage $V$ and current $I$. |
| $(*)_t$ | $(*)$ at $to$ end, $*$ can be voltage $V$ and current $I$. |
| $(*)_{ij}$ | $(*)$ of power line which is connected from bus $i$ to bus $j$. |
| $(*)_i, (*)_j$ | $(*)$ at bus $i$ or $j$. |
| $\mathcal{C}$ | Set for all buses which are connected to centralized reactive power compensation system. |
| $\mathcal{M}$ | Set of load scenarios. |
| $\mathcal{S}$ | MVA flow of power line. |
| $\Delta QC$ | Step increment of reactive power compensation capacity. |
| $\lambda$ | Probability of load situation. |
| $\mu$ | Electricity tariff. |
| $\phi$ | Admittance angle. |
| $\rho$ | Probability of load scenario. |
| $\theta$ | Voltage phase angle. |
| $AOTC$ | Annualized one-time cost of capacitor bank. |
| $B_c$ | Line charging susceptance. |
| $B_{sh}$ | Shunt susceptance. |
| $ETCH$ | Expected total cost per hour of distribution power system. |
| $FC$ | Combined cost of capacitors, installation and cables. |
| $G_{sh}$ | Shunt conductance. |
| $I$ | Current. |
| $i^0$ | Index of buses which are connected to centralized capacitor bank. |
| $Line$ | Number of distribution lines. |
| $lt$ | Capacitor's life time. |

Manuscript received September 20, 2013; revised January 03, 2014, March 17, 2014, and April 29, 2014; accepted May 13, 2014. This work was supported by the Maritime and Port Authority of Singapore , a local Singapore shipyard , and Energy Research Institute at NTU under the LEMS project. Paper no. TPWRS-01213-2013.

S. X. Chen is with DNV GL Energy (formerly KEMA), Singapore (e-mail: nosper@pmail.ntu.edu.sg).

Y. S. Foo. Eddy and H. B. Gooi are with the School of Electrical and Electronic Engineering, Nanyang Technological University, Singapore (e-mail: fooy0027@ntu.edu.sg; ehbgooi@ntu.edu.sg).

M. Q. Wang is with Shandong University, Jinan, China (e-mail: wang0367@sdu.edu.cn).

S. F. Lu is with Xi'an Jiaotong-Liverpool University, Xi'an, China (e-mail: shaofeng.lu1@gmail.com).

Color versions of one or more of the figures in this paper are available online at http://ieeexplore.ieee.org.

Digital Object Identifier 10.1109/TPWRS.2014.2326520

| | |
|---|---|
| $MC$ | Maintenance cost of the capacitor bank. |
| $P$ | Active power. |
| $P_{Loss}$ | Power line loss. |
| $Q$ | Reactive power. |
| $QC$ | Size of centralized capacitor bank. |
| $R$ | Resistance. |
| $r$ | Interest rate. |
| $TCPH$ | Total cost per hour of capacitor bank installed. |
| $TCPL$ | Expected hourly total cost for power loss. |
| $V$ | Voltage. |
| $X$ | Reactance. |
| $Y$ | Admittance. |
| $Y_{series}$ | Line series admittance. |
| $Y_{sh}$ | Shunt admittance. |
| LV | Low voltage. |
| PCC | Point of common coupling. |
| SVC | Static var compensator. |

## I. Introduction

REACTIVE power compensation strategies in power systems help to reduce resistive power losses, control system voltage levels and improve power factors [1]. The static var compensator (SVC) which relies on power electronic control techniques for adaptive reactive power compensation has been widely used in industrial power systems to compensate for large fluctuations in reactive power demand [2]. However, the use of SVC is currently not cost-justifiable in distribution systems. Capacitor banks on the other hand have proved [3] to provide satisfactory cost benefits and are commonly used for passive reactive power compensation in low voltage (LV) distribution systems.

In the past, several capacitor planning methodologies which use homogeneous reactive power load distribution and uniform conductor size along feeders [4]–[6] mainly focus on the optimal placement of reactive power injection. Early analytical methods for capacitor placement are developed by Neagle and Samson [7]. The problem is to determine the optimal location and size of a given number of capacitors such that the system losses are minimized for a given load level. Cook [8] extended the problem formulation to include peak power and energy loss reduction and proposed a method to determine the optimal location and size of the capacitors. Grainger *et al.*[9] have also conducted an extensive research in this area where they proposed several methods including the normalized feeder/load technique. Dynamic programming was also used by Duran [10] to solve the capacitor placement problem. In addition, Haghifam and Malik [11] extended the capacitor placement problem formulation to include the optimal placement of fixed and switchable capacitors in radial distribution networks considering time varying load and load uncertainty based on a proposed genetic algorithm (GA) method.

In [4], Baran and Wu developed a complete problem formulation by modeling the power system through a set of equations with limiting constraints and incorporating an objective function to minimize costs. The problem was then decomposed into optimal placement and optimal sizing problems. By decomposing the problem, the integer part of the problem corresponding to optimal placement is disassociated from the continuous part corresponding to optimal sizing. Furthermore, the problem of starting from an infeasible solution is rarely addressed. This problem is generally overcome by placing capacitors in the power system using the heuristic knowledge of a system planner. In addition, renewable energy and economic dispatch are usually not considered in the problem formulation. Many research works have studied capacitor planning at transmission and distribution voltage levels [12], [13]. A few articles have considered renewable options as part of capacitor planning for LV distribution power systems [3], [14].

If the LV distribution power system has heavy inductive load, it needs a capacitor bank to maintain its power factor at the point of common coupling (PCC) based on the utility grid requirement. Otherwise the consumer will be penalized by the Singapore grid operator if the power factor falls below 0.85. The current industry practice is to locally install a capacitor bank to maintain the local bus voltage and power factor [15], [16]. This paper proposes a new idea by centralizing individual local capacitor banks together to maintain bus voltages and power factors as well as to reduce the power cable loss.

It is also very costly and uneconomical to buy a capacitor bank and install it wherever it is required especially it is used only for a short duration during early morning hours when pumps for dry docks are run. The buses which require reactive power at different time of the day are not always the same. By centralizing all capacitor banks, the total capacity can be shared by each connected bus. It can also help to reduce the total installed capacity of capacitor banks instead of installing individual capacitor banks locally. Besides, the centralized reactive system can be easily expanded to meet any future load increase.

During the planning of reactive power compensation, decentralized methods only provide optimal capacitor placement for a particular load situation. If the load situation changes a new set of optimal capacitor placement will be given by the decentralized method. However during actual operation, it is not practical to keep moving capacitor banks from one location to another according to the load situation. Hence the capacity of the capacitor bank at a location is fixed normally once it has been installed. In addition, capacitor banks at some buses with low load are unable to share their excess capacity of reactive power with other buses that have heavy load. In comparison, the proposed method takes into account the different load situations using a probabilistic approach to classify the bus load groups into different load scenarios. The proposed centralized capacitor bank can also connect to as many buses as they require so there is no need to move the centralized capacitor bank around. The capacity sharing of the centralized reactive power compensation system is also considered in the formulation.

The proposed centralized reactive power compensation system can help to minimize the total cost of capacitors and the

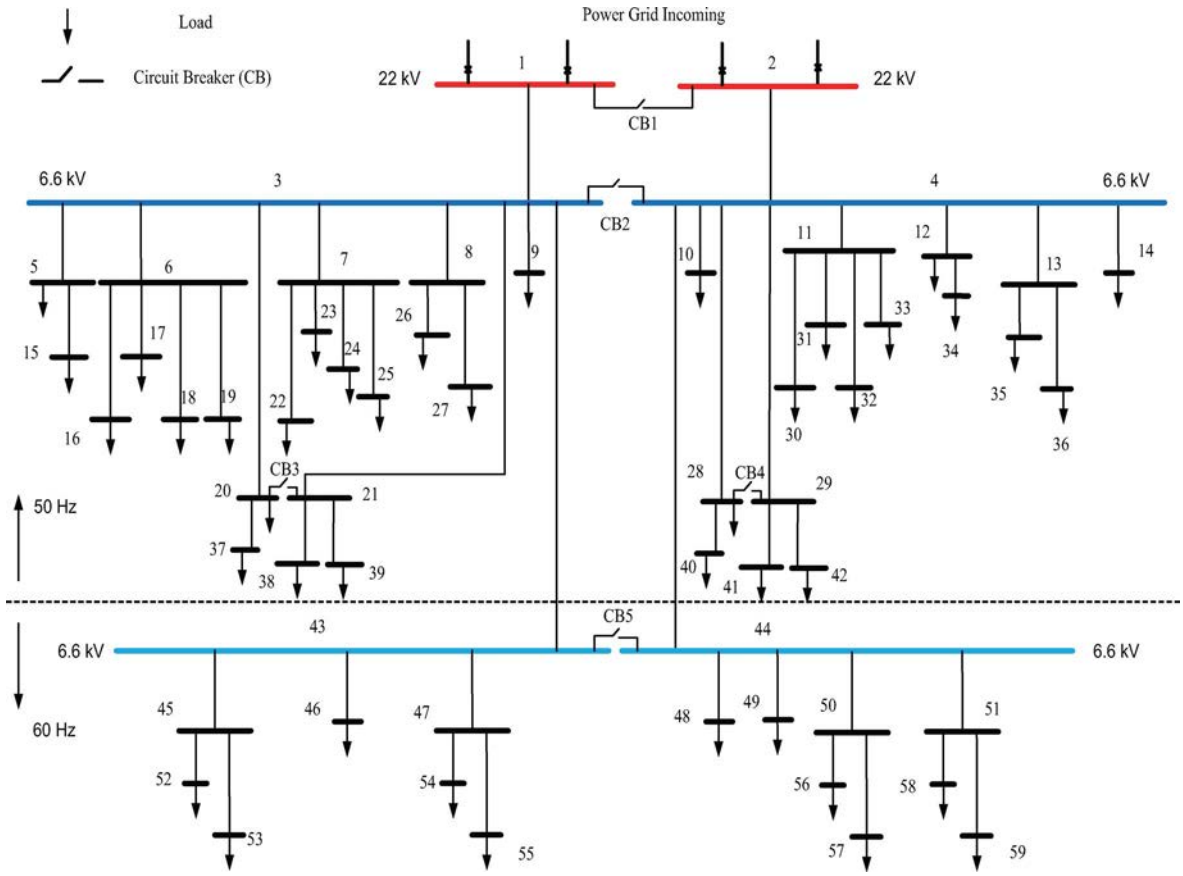


Fig. 1. Example of a distribution power system.

TABLE I
VOLTAGE LEVELS OF 59 BUSES

| Voltage | Bus |
|---|---|
| 22 kV | 1, 2 |
| 6.6 kV | 3-14, 43-45, 47, 50-51 |
| 0.4 kV | 15-42, 46, 48-49, 52-59 |

resistive power cable losses in distribution power systems. The algorithm developed in this paper can help to find an optimal size for the proposed centralized reactive power system where the cost of capacitors and resistive power losses are minimized taking into account the different load situations at every bus in the distribution system.

However, the proposed approach may be effective only for a small LV distribution network because reactive power cannot travel over long distances. This means that the cable length needed by the proposed approach is limited to a few kilometers long. The proposed method has been validated on a real shipyard distribution network having an area of 2 $\mathrm{km}^2$. Simulation results have shown that the proposed method performs well compared to those of the current industry practice.

In Section II, a description of the proposed centralized reactive power compensation system is introduced. The line model of a power system is presented in Section III-A. Formulation for the cost of capacitor placements is provided in Section III-B and the objective function for cost minimization is described in Section III-C. A case study considering a 59-bus power system is tested and the results are shown in Section IV. The optimal size analysis is shown in Section IV-A. A real load situation test is shown in Section IV-B. The conclusion is presented in Section V.

## II. CENTRALIZED REACTIVE POWER COMPENSATION SYSTEM

Reactive power planning of power systems provides the strategy of reactive power compensation so that the real power loss can be reduced and the system voltage profile and power factor can be improved [1]. Compared with SVCs, capacitor banks have satisfactory cost benefits and are widely used in distribution systems. The capacitor banks are chosen for reactive power compensation in this paper. An example of an LV distribution power system is shown in Fig. 1 which features an electrical grid system comprising 59 buses, three voltage levels, i.e., 0.4 kV, 6.6 kV, and 22 kV, and two frequencies, i.e., 50-Hz and 60-Hz of a Singapore shipyard. The voltage level of each bus is shown in Table I. The supply is an inherent 50-Hz system. The 60-Hz system which provides shore power to vessels is converted from the 50-Hz supply via a 6-MVA static frequency converter located at lines 3–43 and 4–44. This shipyard distribution system is used in the case study.

Two key issues have been identified for the optimal placement of capacitor banks at the distribution voltage level. First, the nature of the loads connected to the buses is time varying and exhibits different load patterns throughout the day. It is very difficult to decide the optimal locations and sizing of the capacitor banks for different load situations. Second, capacitor banks

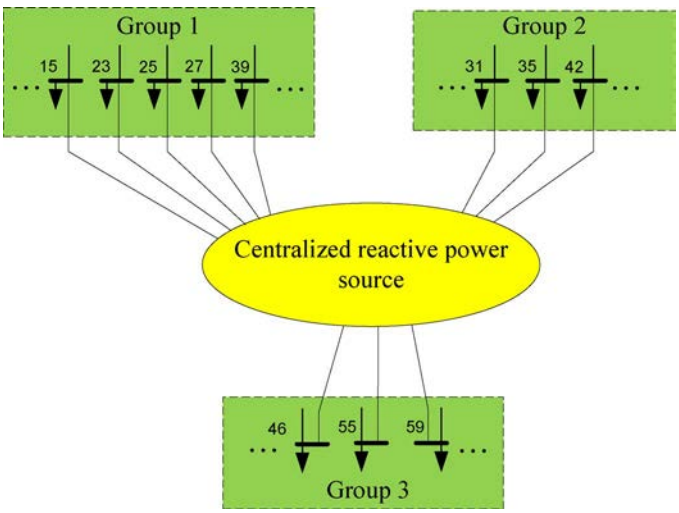


Fig. 2. Centralized reactive power compensation system.

at some buses with low load are unable to provide their excess capacity to other buses with heavy load once they have been placed. Therefore, it is important to address these issues so that the associated costs of the capacitor bank and resistive power losses can be minimized. To solve these problems, a centralized reactive power compensation method is proposed in Fig. 2. The capacitor bank is centralized and can be connected with selected buses where they need reactive power compensation. The total capacity of the centralized capacitor bank can be shared by the connected buses. The objective of the proposed method is only to determine the optimal size of the centralized reactive power compensation system while minimizing the cost of capacitors and resistive power losses for every possible load situations. This will be discussed in the subsequent sections.

Currently the centralized capacitor bank has not been fully implemented in the industry yet. It will be tested in the shipyard distribution power system in Fig. 1 under the land-based energy management systems (LEMS) project. Once the centralized capacitor bank is installed, it will be under the command of an online AC optimal power flow (OPF) function based on the online load information [17], [18]. The OPF function will send the optimal injected reactive power commands to the centralized capacitor bank. The local programmable logic controller (PLC) within the centralized capacitor bank will automatically change its outputs to each connected bus.

The load profile changes according to different periods of the day resulting in peak and valley periods which may differ for each load bus. However, some buses are coherent where the connected loads share the similar peak and valley periods which can be classified as a group. Consequently, the distribution power system can be categorized into different load groups where each load group shares similar peak and valley periods.

The load group can be classified by relative electrical distance (RED) [19], load type or historical load data. The last two are used to help to classify the load group in this paper. The load type and historical load data can tell us which bus needs reactive power support and those buses that can be connected with the centralized reactive power compensation system. The possible buses which need to be connected with the centralized reactive power compensation system in Fig. 1 are buses 15, 23, 25, 27, 31, 35, 39, 42, 46, 55, and 59 based on the load type and historical load studies. These buses are shown in Fig. 2. Besides, buses which are connected with the same load type and share the similar peak and valley periods based on the historical load data can be classified as the same load group.

TABLE II
CLASSIFICATION OF LOAD

| Group | Bus |
|---|---|
| 1 | 5-9, 15-27, 37-39 |
| 2 | 10-14, 28-36, 40-42 |
| 3 | 45-59 |

In this paper, all the buses in Fig. 1 have been classified into three major groups based on their load types and historical load data. They are shown in Table II. Buses within the same group share common characteristics such as close proximity with each other and similar load profiles.

The variation of a load can be categorized into different ranges, i.e., the load has a maximum value during the peak period and a minimum value during the valley period. In a distribution system, most buses will have two states, i.e., loaded or unloaded. For simplicity, two average values are used to represent each load's situation. The first average value represents the low load situation at bus $i$ and is defined as $P_i^L$. The second average value represents the high load situation and is defined as $P_i^H$. In addition, the probabilities of $P_i^L$ and $P_i^H$ are defined as $\lambda_i^H$ and $\lambda_i^L$. The relationship of these two probability values is shown in (1):

$$\lambda_i^H + \lambda_i^L = 1. \tag{1}$$

## III. Distribution System Modeling and Problem Formulation

### A. Line Models

Fixed loads are modeled as constant real and reactive power injections, $P_D$ and $Q_D$. The shunt admittance of any constant impedance shunt elements at a bus is specified by $G_{sh}$ and $B_{sh}$. Hence, the bus shunt matrix element, $Y_{sh} = G_{sh} + jB_{sh}$ is introduced.

Each distribution line is modeled as a standard $\pi$, with a series resistance $R$ and a reactance $X$ and one half of the total line charging susceptance $B_c$ at each end of the line. $B_c$ is the inverse of the line charging capacitance $x_c$. The line charging capacitance is not considered in the case study of the shipyard distribution power network due to the short cable length. The model is shown in Fig. 3 [20]. Branch voltages and currents from the $from$ end to the $to$ end of the distribution line $l$ are related by the branch matrix $Y^l$ as follows:

$$\begin{bmatrix} I_f^l \\ I_t^l \end{bmatrix} = Y^l \begin{bmatrix} V_f^l \\ V_t^l \end{bmatrix} \tag{2}$$

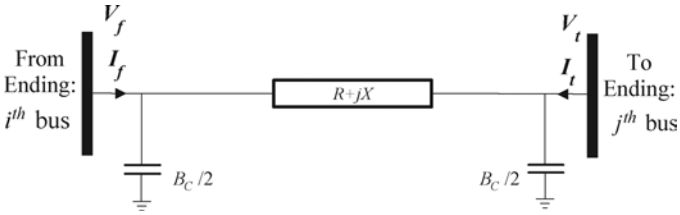


Fig. 3. Simple line model in a power system.

where $Y^l = \begin{bmatrix} (Y_{series} + jB_c/2) & -Y_{series} \\ -Y_{series} & Y_{series} + jB_c/2 \end{bmatrix}$ and $Y_{series} = 1/(R + jX)$.

### B. Cost of Capacitors

The cost incurred in installing new capacitors includes a one-time cost and a maintenance cost. The one-time cost is proportional to the size of capacitors. Hence the one-time cost of installing a capacitor of size $QC$ (*Mvar*) would be $QC * FC$, where $FC$ (*$/Mvar*) is the combined cost of capacitors, installation and cables. The maintenance cost per year is also proportional to the size of capacitors. If the capacitor's life time is $lt$ years and the maintenance cost is $MC$ (*$/Mvar*) per year, then the total cost of the capacitors is $(QC * FC + lt * QC * MC)$ ($).

The total payment for all the capacitors in $lt$ years will be normalized in *$/hr*, which is suitable for the short term study. If the interest rate $r$ for financing the installed capacitors is considered, the annualized one-time cost ($AOTC$) for the capacitors is shown in (3):

$$AOTC = \frac{r(1+r)^{lt}}{(1+r)^{lt}-1}(QC * FC). \quad (3)$$

The total cost of the capacitor bank can be obtained by adding $AOTC$ and the maintenance cost together. Then the total cost per hour ($TCPH$) of the capacitor bank installed can be found in (4):

$$TCPH = \frac{1}{8,760} * (AOTC + QC * MC). \quad (4)$$

### C. Objective Function of Cost Minimization

The total cost for the distribution power system includes the payment of the total electricity bill and the cost of capacitors. Considering the different load situations, the electricity bill payment of the total power line loss is also not the same for every hour. Hence, the expected total cost per hour ($ETCH$) is proposed here only to express the equivalent variable cost per hour of the distribution power system. It includes the expected hourly total cost for the power loss ($TCPL$) and hourly cost of capacitors ($TCPH$).

There are two electricity tariffs for the distribution power system in Singapore [21], namely high tariff and low tariff. High tariff $\mu^H$ is used for the on-peak period and low tariff $\mu^L$ is used for the off-peak period. In this paper, $\mu^H$ will be used when the supply system is under high load situations. $\mu^L$ will be used when the supply system is under low load situations.

Table III shows all scenarios in Set $\mathcal{M}$ for the shipyard power system in Fig. 1. The bus in each group will have similar high/low load situations and they share the same on-peak or off-peak period. The group details can be found in Table II. If the load situation in one group lies in the on-peak period, it is classified as high load and the probability of this group in this scenario is $\lambda^H$. Otherwise the probability of this group in this scenario is $\lambda^L$. There are three load groups in the shipyard power system in Fig. 1. Hence, there are eight scenarios of different load combinations. As shown in Table III, scenarios 1–4 are under high load situations, which correspond to high electricity tariff $\mu^H$. Scenarios 5–8 are under low load situations, which correspond to low electricity tariff $\mu^L$.

TABLE III
DIFFERENT LOAD SCENARIOS IN SET $\mathcal{M}$

| Set $\mathcal{M}$ | Load situation[a] Group 1 | Group 2 | Group 3 | Probability $\rho^s$ | Electricity tariff $\mu^s$ |
|---|---|---|---|---|---|
| 1 | High | High | High | $\lambda^H * \lambda^H * \lambda^H$ | $\mu^H$ |
| 2 | Low | High | High | $\lambda^L * \lambda^H * \lambda^H$ | $\mu^H$ |
| 3 | High | Low | High | $\lambda^H * \lambda^L * \lambda^H$ | $\mu^H$ |
| 4 | High | High | Low | $\lambda^H * \lambda^H * \lambda^L$ | $\mu^H$ |
| 5 | Low | Low | High | $\lambda^L * \lambda^L * \lambda^H$ | $\mu^L$ |
| 6 | Low | High | Low | $\lambda^L * \lambda^H * \lambda^L$ | $\mu^L$ |
| 7 | High | Low | Low | $\lambda^H * \lambda^L * \lambda^L$ | $\mu^L$ |
| 8 | Low | Low | Low | $\lambda^L * \lambda^L * \lambda^L$ | $\mu^L$ |

[a] The bus in each group will have High/Low load situations.

Considering different load scenarios in Table III, the $ETCH$ can be expressed as

$$Minimize: ETCH = \sum_{s \in \mathcal{M}} \rho^s \{TCPL^s + TCPH^s\} \quad (5)$$

where $\mathcal{M}$ is a set of different load scenarios as shown in Table III. $TCPL^s = \mu^s * P^s_{Loss}$, where $\mu^s$ is the electricity tariff during load scenario $s$ and $P^s_{Loss}$ is the active power line loss for scenario $s$. $\rho^s$ is the probability of scenario $s$, and $TCPH^s$ is the total capacitor cost per hour for scenario $s$. $ETCH$ is defined as the sum of the cost of each scenario times their probability.

The probability $\rho^s$ of scenario $s$ is defined as the product of probabilities of three load groups. The electricity tariff $\mu^s$ is $\mu^H$ or $\mu^L$ based on the load situations of scenario $s$. For example, in scenario 1, the load situations of all groups are high. The probability $\rho^1$ is $\lambda^H * \lambda^H * \lambda^H$ and the electricity tariff $\mu^1$ is $\mu^H$.

The active power line loss in (5) can be expressed as

$$P^s_{Loss} = \sum_{l=1}^{Line} |real(V_f^{l^s}(I_f^{l^s})^* - V_t^{l^s}(I_t^{l^s})^*)| \; \forall s \quad (6)$$

where $V_f^{l^s}$, $I_f^{l^s}$, $V_t^{l^s}$, and $I_t^{l^s}$ are voltages and currents at the $from$ bus, $f$, and the $to$ bus, $t$, of distribution line $l$ during scenario $s$, respectively. $(I_f^{l^s})^*$ and $(I_t^{l^s})^*$ are the conjugate variables of $I_f^{l^s}$ and $I_t^{l^s}$, respectively.

To solve the objective function of (5), the following constraints need to be considered.

*1) Active Power Balance [22]:*

$$P_i^{G^s} - P_i^{D^s} = P_i^s = V_i^s \sum_j V_j^s Y_{ij} \cos(\theta_i^s - \theta_j^s - \phi_{ij}^s) \; \forall i, j, s \quad (7)$$

where $P_i^{G\,s}$ is the injected active power at bus $i$ during scenario $s$, which includes the conventional and renewable energy. $P_i^{D\,s}$ is the active load power at bus $i$ and $P_i^s$ is the active power transferred out from bus $i$. Bus $i$ is connected to bus $j$ via line $ij$. $\theta_i^s$ and $\theta_j^s$ are the respective voltage phase angles at buses $i$ and $j$ during scenario $s$. $\phi_{ij}^s$ is the admittance angle of $Y_{ij}$ during scenario $s$.

*2) Reactive Power Balance:* For bus $i$ which is not connected with the centralized capacitor bank

$$\begin{aligned} Q_i^{G\,s} - Q_i^{D\,s} &= Q_i^s \\ &= V_i^s \sum_j V_j^s Y_{ij} \sin(\theta_i^s - \theta_j^s - \phi_{ij}^s)\ \forall j, s \end{aligned} \quad (8)$$

where $Q_i^{D\,s}$ is the reactive load at bus $i$ and $Q_i^s$ is the reactive power transferred out from bus $i$. $Q_i^{G\,s}$ is the injected reactive power of the generator or upstream grid at bus $i$.

For bus $i^0$ which is connected with the centralized capacitor bank

$$\begin{aligned} Q_{i^0}^{C\,s} - Q_{i^0}^{D\,s} &= Q_{i^0}^s \\ &= V_{i^0}^s \sum_j V_j^s Y_{i^0 j} \sin(\theta_{i^0}^s - \theta_j^s - \phi_{i^0 j}^s)\ \forall j, s \end{aligned} \quad (9)$$

where $Q_{i^0}^{C\,s}$ is the reactive power injected by the centralized capacitor bank at bus $i^0$; $Q_{i^0}^{D\,s}$ is the reactive load at bus $i^0$; and $Q_{i^0}^s$ is the reactive power transferred out from bus $i^0$. $\theta_{i^0}^s$ is the voltage phase angle at bus $i^0$ during scenario $s$. $\phi_{i^0 j}^s$ is the admittance angle of $Y_{i^0 j}$ during scenario $s$.

The capacity limit of the centralized reactive power compensation system is

$$\sum_{i^0 \in \mathcal{C}} Q_{i^0}^{C\,s} \le QC\ \forall s \quad (10)$$

where $\mathcal{C}$ is the set for all the buses which are connected with the centralized reactive power compensation system. $QC$ is the capacity of the centralized reactive power compensation system.

Equations (8)–(10) address the reactive power injection from the centralized reactive power compensation system.

The MVA flow of power lines and bus voltages are

$$\begin{aligned} \mathcal{S}_{ij}^s &\le \mathcal{S}_{ij}^{\max}\ \forall i, j, s \\ (V_i^s)^{\min} &\le V_i^s \le (V_i^s)^{\max}\ \forall i, s \end{aligned} \quad (11)$$

where $\mathcal{S}_{ij}^s$ is the MVA flow of the power line which is connected from bus $i$ to bus $j$ during scenario $s$. $\mathcal{S}_{ij}^{\max}$ is the capacity limit of the power line which is connected from bus $i$ to bus $j$. $(V_i^s)^{\min}$ and $(V_i^s)^{\max}$ are the minimum and maximum voltage requirement for bus $i$ during scenario $s$.

### D. Solution Algorithm

The objective function in (6) is to minimize the ETCH under a fixed $QC$. The control variables are the injected reactive power to each connected bus. These buses are 15, 23, 25, 27, 31, 35, 39, 42, 46, 55, and 59 as shown in Fig. 2. The solution process starts with a minimum QC required by the LV distribution power system. After that, $QC$ will be increased by a step size and the $ETCH$ is minimized again. In this manner, the optimal size of $QC$ can be found by identifying the minimum value among all the minimized ETCH computed at each step.

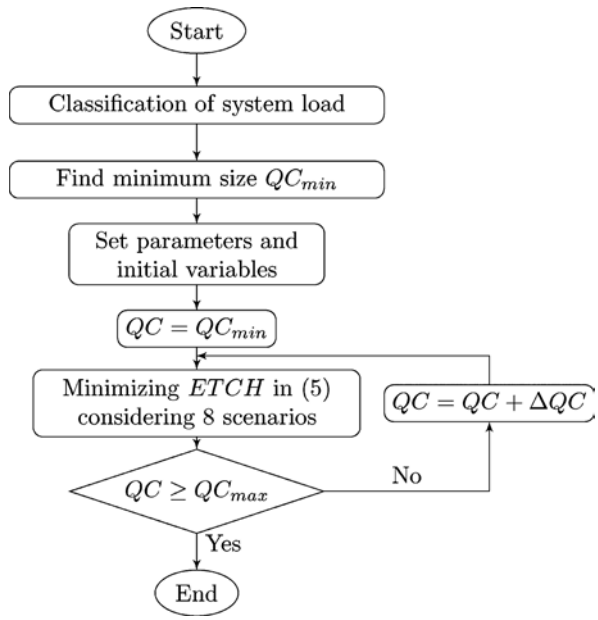


Fig. 4. Algorithm used to solve the optimal capacity of centralized reactive power compensation system.

$QC$ can also be considered as a variable with an upper and lower limit. However, there are two main concerns: Firstly, the optimization problem in (5) is a highly complex nonlinear optimization problem and it includes eight AC OPF (optimal power flow) problems corresponding to the eight scenarios in Table III. It may not be able to find a converged solution for this optimization problem if $QC$ is considered as an additional variable in (5). Secondly, the detailed relationship between ETCH and $QC$ cannot be established when $QC$ is considered as a variable. $QC$ is not a continuous value in reality since the switched capacitance is a discrete value and 0.10 *Mvar* may be considered as the step increment.

Fig. 4 shows the developed algorithm which is used to solve the optimal size of the centralized reactive power compensation system. This algorithm will compute different $ETCH$s for different sizes of the centralized reactive power compensation system that lie in between the minimum size $QC_{\min}$ and maximum size $QC_{\max}$. The minimum size $QC_{\min}$ of the distribution power system is the minimum value to make the power flow calculation converged under the voltage limits. For all the scenarios, they have different minimum sizes $QC_{\min}^s$ based on their different load situations. The value of $QC_{\min}$ for the distribution power system will be the maximum value among these different minimum sizes of different load situations. The maximum size $QC_{\max}$ of the distribution power system is constrained by the investment fund available for the capacitor bank purchase and the space to house the capacitor bank. Normally it can be set as a relative large value. The optimal size for the distribution power system can then be found by identifying the minimum cost of (5).

The details of this algorithm are as follows:

1) Enter the load and network information. Find the minimum capacity $QC_{\min}$ of the centralized reactive power compensation system by power flow calculations.
2) Classify the load into different load groups based on their load types and historical load data.
3) Set $QC_{\max}$, which is relatively large for the distribution power system, $\Delta QC$ for each step increment of the reactive power compensation and the unit and system parameters. Initialize all the variables used.
4) Solve the objective function for $QC$, which is the size of the centralized reactive power compensation system. Minimize $ETCH$ in (5) considering the probability of each scenario for the distribution power system.
5) If $QC < QC_{\max}$, update $QC$ using $QC = QC + \Delta QC$ and go to step 4. The algorithm will stop when $QC \geq QC_{\max}$.

The proposed solution is a nonlinear problem. This algorithm is implemented in AMPL (A Modeling Language for Mathematical Programming) [23] with KNITRO, a nonlinear optimization solver [24].

## IV. Cost-Benefit Analysis—Case Studies

This section attempts to determine the optimal size of the centralized reactive power compensation system for the distribution power system which is shown in Fig. 1. The probability of different load situations are considered in the eight scenarios as shown in Table III. The two electricity tariffs for the distribution power system in Singapore are also considered in this paper. The high tariff $\mu^H$ used for the distribution power system in Singapore is \$0.2124/*kWh* and the low tariff $\mu^L$ used is \$0.1314/*kWh* [21].

The interest rate $r$ for financing the installed centralized reactive power compensation system is set at 6%. The one time cost for the capacitor bank of $100\ kvar$, cables and installation is about \$7500 and the maintenance cost for that capacitor bank is \$750 [25]. The lifetime of a capacitor bank is set to 5 years. For the power distribution system of the local shipyard, the minimum capacity $QC_{\min}$ for the power flow calculation to converge was found to be 8.90 *Mvar*. The maximum capacity $QC_{\max}$ was set at 16.50 *Mvar*. The probability $\lambda_i^H$ of the high load situation and the probability $\lambda_i^L$ of the low load situation are set as 0.7 and 0.3, respectively. The maximum and the minimum voltage limits are set as 1.05 *pu* and 0.95 *pu*. The capacity limit of the power line connected to the centralized reactive power compensation system is 1.5 *MVA*.

In the distribution power system of Fig. 1, the possible buses which need to be connected with the centralized reactive power compensation system are buses 15, 23, 25, 27, 31, 35, 39, 42, 46, 55, and 59 as shown in Fig. 2. The area of this shipyard power system is about 2 $\mathrm{km}^2$ and the centralized reactive power compensation system is located at the central area, which is easier to be connected with those buses. The parameters of the cables connecting the capacitor banks can be found in [26]. These bus numbers are decided based on the historical load data.

The high/low active and reactive load values at each bus in this 59-bus distribution power system can be found in [27] and [28]. The branch parameters can be found in [29].

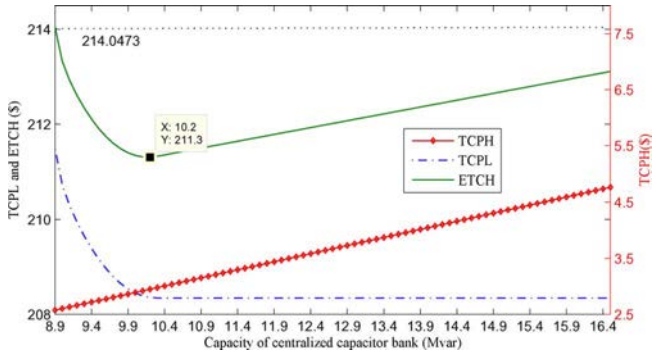


Fig. 5. Cost comparison for the shipyard distribution power system.

### A. Analysis of Optimal Capacitor Size

The proposed solution algorithm has been solved and the computed values of $TCPL$, $TCPH$, and $ETCH$ were plotted with respect to the capacity of the centralized capacitor bank $QC$ for cost comparison as shown in Fig. 5. The minimum capacity $QC_{\min}$ is 8.90 *Mvar* and the maximum capacity $QC_{\max}$ is 16.50 *Mvar*. $QC$ is not a continuous value in reality since the switched capacitance is a discrete value and the proposed solution algorithm is performed with a step size of 0.10 *Mvar*. At each step, the proposed solution algorithm minimizes $TCPL$ and $ETCH$ by considering all the eight scenarios in Table III.

From Fig. 5, the initial value of $TCPH$ is evaluated to be \$2.57 while $TCPL$ is \$211.48 and ETCH is \$214.05 based on $QC_{\min}$. At $QC_{\max}$, the maximum value of $TCPH$ is computed to be \$4.77 while $TCPL$ is \$208.30 and ETCH is \$213.07. It is observed that $TCPH$ exhibits an upward linear trend revealing that the increase in capacitor bank capacity results in higher costs. This agrees with (4), where for the given $MC$, $FC$, $r$, and $lt$, $TCPH$ has a linear relationship with $QC$. Conversely, $TCPL$ has a downward trend with respect to $QC$. This is expected since a higher capacitor bank capacity reduces the power loss in the system. However, it can be seen that the value of $TCPL$ begins to saturate at \$208.30 when $QC$ is about 10.20 *Mvar* and the saturation trend happens for any other power systems based on the voltage limitation. This shows that the power loss in the shipyard distribution power system can only be reduced to a certain value beyond which a further increase in $QC$ does not yield a further reduction in power loss of the system. It can be seen that $ETCH$ exhibits a trend with two distinct regions. The first region shows the value of $ETCH$ decreasing up to the point where $QC$ is 10.20 *Mvar*. The second region shows the value of $ETCH$ increasing for $QC$ greater than 10.20 *Mvar*. The lowest value for $ETCH$ is found to be \$211.30 which corresponds to 10.20 *Mvar*, the capacity of the centralized capacitor bank. It is also observed that the optimal value of $QC$ occurs when $TCPL$ begins to reach a steady state value. The optimal size of the centralized capacitor bank is obtained when $QC$ yields the lowest value of $ETCH$. This value is 10.20 *Mvar* and it lies between $QC_{\min}$ and $QC_{\max}$.

Based on the different load scenarios in Set $\mathcal{M}$ of Table III, a pie chart consisting of the expected load distribution for all scenarios is shown in Fig. 6(a). The expected load (*MVA*) of each scenario is defined as all the load of this scenario times

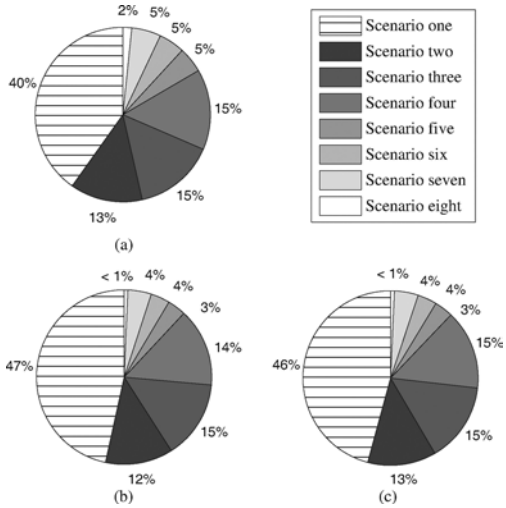


Fig. 6. Proportion of demand and power loss for all scenarios. (a) Expected load (MVA) distribution for all scenarios. (b) Expected power loss distribution for all scenarios at the initial capacity of capacitor banks. (c) Expected power loss distribution for all scenarios at the optimal capacity of capacitor banks.

the probability of this scenario. The total expected load of all scenarios is defined as the sum of the expected load (*MVA*) of each scenario. The load data of each scenario serves as input for the minimization of $ETCH$ during each step change in $QC$. The load distribution percentages of each scenario are derived by using the expected load (*MVA*) of each scenario divided by the total expected load of all scenarios in Set $\mathcal{M}$.

Fig. 6(b) and (c) shows the pie chart of the expected power loss distribution at the initial capacity and at the optimal capacity of the centralized capacitor bank for all scenarios, respectively. The expected power loss of each scenario is defined as the power loss of this scenario times the probability of this scenario. The total expected power loss of all scenarios is defined as the sum of the expected power loss of each scenario. The total expected power loss at the initial and optimal capacity of the capacitor bank are 1.0432 *MW* and 1.0285 *MW*, respectively. At the optimal capacity, there is a reduction of 1% in the expected power loss distribution for scenario one while an increase of 1% in the expected power loss distribution is observed for scenarios two and four. Although an increase in the expected power loss distribution for scenarios two and four is observed, the magnitude of the actual power loss at the optimal capacity for each scenario is significantly smaller than that of the initial capacity. In addition, the expected power loss distribution has a similar composition compared to that of the expected load distribution. This shows that the expected power loss is proportional to the expected load distribution of each scenario. A high load situation contributes to a higher power loss in the system and vice versa.

The expected voltage profile for the 59-bus distribution system at the optimal capacity of the centralized capacitor bank is shown in Fig. 7. For each bus, three different voltage values namely the expected voltage, highest voltage and lowest voltage are shown. The expected voltage for each bus is obtained by multiplying the voltages for each scenario with the corresponding probabilities in Table III and adding them up. The expected voltage is indicated by an asterisk. The highest

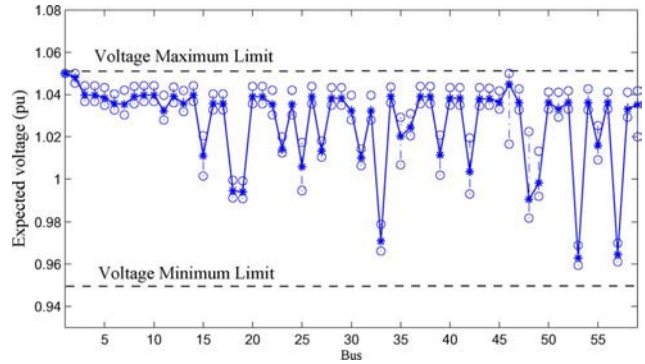


Fig. 7. Expected voltages for 59 buses at the optimal capacity of the centralized capacitor bank.

and lowest voltage values for each bus among all the scenarios are indicated by a circle. The highest and lowest voltage values of each bus are chosen from all the possible values of all the scenarios. The highest and lowest voltage values for each bus are within the maximum and minimum voltage limits for all scenarios. The expected voltage profile for each bus also satisfies the minimum and maximum voltage limits.

The expected injected reactive power profile for the selected buses at the optimal capacity of the centralized capacitor bank is shown in Fig. 8. In this study, buses connected to the centralized capacitor bank are buses 15, 23, 25, 27, 31, 35, 39, 42, 46, 55, and 59. For each of the selected buses, three different injected reactive power values namely the expected injected reactive power, highest and lowest injected reactive power are shown. The expected injected reactive power is obtained by multiplying the injected reactive power for each scenario with the corresponding probabilities and adding them up. The injected reactive power for each scenario is calculated from the optimization problem in (5) under the constraints (6)–(11). The optimization algorithm will help to decide the optimal injected reactive power for each connected bus based on the AC OPF calculation for each scenario. The expected injected reactive power is indicated by an asterisk. The highest and lowest injected reactive power values for each bus among all the scenarios are indicated by a circle. It is observed that the highest, lowest and expected injected reactive power for each of the selected buses is within the *MVA* limit of the power line connected to the centralized capacitor bank in Fig. 8.

To further explain Fig. 8, the injected reactive power at bus 15 for the eight scenarios is shown in Table IV. The third column shows the injected reactive power for each scenario which is decided by AC OPF. The highest and lowest injected reactive power values are found to be 0.90 *Mvar* in scenario 1 and 0.24 *Mvar* in scenario 8 respectively. The expected injected reactive power of bus 15 can be calculated by multiplying the third column with the second column of Table IV and adding them up, which is found to be 0.6052 *Mvar*. Likewise, the expected injected reactive power for the other buses can be determined in a similar way.

### *B. Real Load Situation Test*

The real load situation for the distribution power system in Fig. 1 is applied here to check the performance of the central-

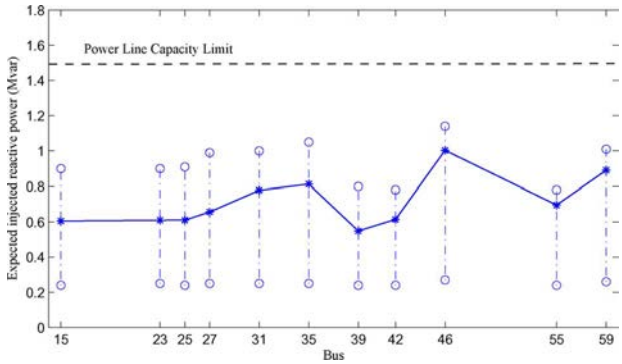


Fig. 8. Expected injected reactive power at the optimal capacity of the centralized capacitor bank.

TABLE IV
INJECTED REACTIVE POWER AT BUS 15 FOR DIFFERENT SCENARIOS

| Set $\mathcal{M}$ | Probability | $Mvar$ |
|---|---|---|
| Scenario 1 | 0.7*0.7*0.7 | 0.90 |
| Scenario 2 | 0.3*0.7*0.7 | 0.25 |
| Scenario 3 | 0.7*0.3*0.7 | 0.65 |
| Scenario 4 | 0.7*0.7*0.3 | 0.61 |
| Scenario 5 | 0.3*0.3*0.7 | 0.25 |
| Scenario 6 | 0.3*0.7*0.3 | 0.25 |
| Scenario 7 | 0.7*0.3*0.3 | 0.58 |
| Scenario 8 | 0.3*0.3*0.3 | 0.24 |

ized reactive power compensation system at the optimal size of 10.2 *Mvar*. Under one real load situation [30], there are 11 buses installed with the local capacitor banks which try to maintain the voltage level and power factor within the acceptable operating range. The location and size of the installed capacitor banks are decided by the decentralized method based on an average historical load during the planning stage and the results are obtained from the PowerWorld simulation software. The locations of these 11 buses are the same as those buses which are connected to the centralized capacitor bank, i.e., buses 15, 23, 25, 27, 31, 35, 39, 42, 46, 55, and 59. The amount of reactive power required at each of the eleven pre-selected buses ranges from 0.27 Mvar to 1 Mvar which are obtained from PowerWorld. Therefore, a local capacitor bank of 1 Mvar is placed at each of the eleven pre-selected bus to ensure that there is sufficient capacity for the decentralized reactive power compensation.

Table V compares the results obtained from the decentralized method and proposed method. Three different sets of results are compared. The first set of results shows the amount of injected reactive power from the capacitors. Under the decentralized method, a local capacitor bank of 1 *Mvar* is placed at each of preselected buses and the amount of injected reactive power at the respective buses is decided by OPF. For the proposed method, the optimal size of the centralized reactive power compensation system is found to be 10.2 *Mvar* as shown in Fig. 5 and the amount of injected reactive power at the respective buses is also decided by OPF. In comparison, the decentralized method requires a total capacity of 11 *Mvar* while the proposed method requires 10.2 *Mvar*. This shows that the proposed method requires a lesser capacity for reactive power compensation which means a lower installation cost. The second set of

TABLE V
COMPARISON BETWEEN DECENTRALIZED METHOD AND PROPOSED METHOD

| | Decentralized method | | | Proposed method | | |
|---|---|---|---|---|---|---|
| | Bus | Local capacity | Injected Q | Bus | Shared capacity | Injected Q |
| Q from capacitors ($Mvar$) | 15 | 1 | 0.28 | 15 | 10.2 | 0.25 |
| | 23 | 1 | 0.31 | 23 | | 0.34 |
| | 25 | 1 | 0.27 | 25 | | 0.25 |
| | 27 | 1 | 0.27 | 27 | | 0.25 |
| | 31 | 1 | 0.97 | 31 | | 1.00 |
| | 35 | 1 | 0.95 | 35 | | 1.05 |
| | 39 | 1 | 0.29 | 39 | | 0.25 |
| | 42 | 1 | 0.76 | 42 | | 0.78 |
| | 46 | 1 | 1.0 | 46 | | 1.13 |
| | 55 | 1 | 0.90 | 55 | | 0.86 |
| | 59 | 1 | 0.93 | 59 | | 1.01 |
| Q from grid ($Mvar$) | 1.04 | | | 0.81 | | |
| Power loss ($MW$) | 1.085 | | | 0.93 | | |

results compares the amount of reactive power from the grid. It can be seen that the decentralized method requires 1.04 *Mvar* from the grid which is higher than the proposed method of 0.81 *Mvar*. This shows that the proposed method can help the shipyard improve the total power factor at the PCC. The third set of results show that if we replace all the local capacitor banks under the decentralized method with the 10.2 *Mvar* proposed centralized reactive power compensation system, the cable power loss will be reduced from 1.085 *MW* to 0.93 *MW*.

One notable difference between both methods is in the amount of reactive power that can be injected at each bus. Under the decentralized method, a local capacity of 1 *Mvar* is placed at each of the eleven buses and the total reactive power capacity is 11 *Mvar*. If OPF requires the amount of injected reactive power at one of the buses to be more than 1 *Mvar* then the decentralized method will be unable to realize it. However for the proposed method, the amount of injected reactive power at each of the eleven buses can be more than 1 *Mvar* as long as the optimal centralized capacitor bank which is found to be 10.2 *Mvar* has the capacity to be shared among these buses. Therefore, the proposed method is more flexible in terms of the sharable amount of reactive power that can be injected at each bus while the local installed capacitor bank of the decentralized method limits the amount of injected reactive power at that bus.

Compared with the decentralized method, the power loss reduction for the centralized reactive power compensation system is about 14.3%. The injected reactive power distribution for the centralized reactive power compensation system is shown in Fig. 9. The injected reactive power percentages of different buses are calculated by using the injected reactive power at each connected bus divided by the capacity of the centralized reactive power compensation system. The different parts of the pie chart represent the injected reactive power percentages of different buses. The total injected reactive power is 7.17 *Mvar* for all the buses connected with the centralized reactive power compensation system. If the load situation becomes heavier the next moment, the reactive power capacity not used can be shared with any bus which is connected with the centralized reactive power compensation system.

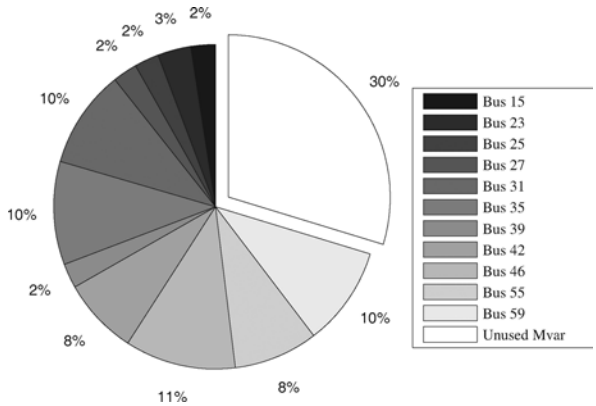


Fig. 9. Injected reactive power distribution at the optimal capacity of centralized capacitor banks under a normal load situation.

## V. Conclusion

A proposed centralized reactive power compensation method has been developed to handle different load situations for distribution power systems in this paper. It aims at overcoming the problems of optimal capacitor placement as well as optimizing the use of capacitor banks under different load situations. A case study was done on a local shipyard consisting of a 59-bus distribution power system. The optimal size of the centralized capacitor bank for the shipyard was found by minimizing $ETCH$ subject to system constraints. The minimal costs of capacitor bank and power loss are obtained by adopting the proposed method. The voltage and injected reactive power profiles obtained also satisfy all system, line and bus constraints. The proposed method was applied in a real load situation and the results are compared with those of local capacitor banks. The results show that there is a significant power loss reduction when adopting the proposed method and the spare capacity of the centralized system can be shared and used by any connected buses to cater for heavier load situations. Besides, it is also very easy to expand the capacity of the centralize reactive power compensation system for future load increase.

The goals of reactive power compensation for distribution power systems under different load situations can be achieved by proposing the centralized reactive power compensation method. It is believed that the proposed method can help to minimize the expected total cost $ETCH$ in the distribution power system.

## Acknowledgment

The authors would like to thank the Microgrid project team of the Clean Energy Research Laboratory for the support rendered.

## References

[1] T. Miller, *Reactive Power Control in Electric System*. New York, NY, USA: Wiley, 1982.

[2] H. Jin, G. Goos, and L. Lopes, "An efficient switched-reactor-based static var compensator," *IEEE Trans. Ind. Appl.*, vol. 30, no. 4, pp. 998–1005, 1994.

[3] S. Chen and H. Gooi, "Capacitor planning of power systems with wind generators and PV arrays," in *Proc. IEEE TENCON 2009 Conf.*, 2009, pp. 1–5.

[4] M. Baran and F. Wu, "Optimal sizing of capacitors placed on a radial distribution system," *IEEE Trans. Power Del.*, vol. 4, no. 1, pp. 735–743, Jan. 1989.

[5] M. Baran and F. Wu, "Optimal capacitor placement on radial distribution systems," *IEEE Trans. Power Del.*, vol. 4, no. 1, pp. 725–734, Jan. 1989.

[6] C. Chen, C. Hsu, and Y. Yan, "Optimal distribution feeder capacitor placement considering mutual coupling effect of conductors," *IEEE Trans. Power Del.*, vol. 10, no. 2, pp. 987–994, Apr. 1995.

[7] N. M. Neagle and D. R. Samson, "Loss reduction from capacitors installed on primary feeders," *IEEE Trans. Power App. Syst.*, vol. PAS-75, no. 3, pp. 950–959, 1956.

[8] R. Cook, "Optimizing the application of shunt capacitors for reactive-volt-ampere control and loss reduction," *IEEE Trans. Power App. Syst.*, vol. PAS-80, no. 3, pp. 430–441, 1961.

[9] J. J. Grainger, S. H. Lee, A. M. Byrd, and K. N. Clinard, "Proper placement of capacitors for losses reduction on distribution primary feeders," in *Proc. Amer. Power Conf.*, Dec. 2006, pp. 342–347.

[10] H. Dura, "Optimum number, location, and size of shunt capacitors in radial distribution feeders a dynamic programming approach," *IEEE Trans. Power App. Syst.*, vol. PAS-87, no. 9, pp. 1769–1774, Sep. 1968.

[11] M. R. Haghifam and O. P. Malik, "Genetic algorithm-based approach for fixed and switchable capacitors placement in distribution systems with uncertainty and time varying loads," *IET Gener., Transm., Distrib.*, vol. 1, no. 2, pp. 244–252, Mar. 2007.

[12] J. Y. Park, J. M. Sohn, and J.-K. Park, "Optimal capacitor allocation in a distribution system considering operation costs," *IEEE Trans. Power Syst.*, vol. 24, no. 1, pp. 462–468, Feb. 2009.

[13] V. Farahani, B. Vahidi, and H. Abyaneh, "Reconfiguration and capacitor placement simultaneously for energy loss reduction based on an improved reconfiguration method," *IEEE Trans. Power Syst.*, vol. 27, no. 2, pp. 587–595, May 2012.

[14] A. Dukpa, B. Venkatesh, and L. Chang, "Fuzzy stochastic programming method: Capacitor planning in distribution systems with wind generators," *IEEE Trans. Power Syst.*, vol. 26, no. 4, pp. 1971–1979, Nov. 2011.

[15] G. Levitin, A. Kalyuzhny, A. Shenkman, and M. Chertkov, "Optimal capacitor allocation in distribution systems using a genetic algorithm and a fast energy loss computation technique," *IEEE Trans. Power Del.*, vol. 15, no. 2, pp. 623–628, Apr. 2000.

[16] H. D. Chiang, J. C. Wang, O. Cockings, and H. D. Shin, "Optimal capacitor placements in distribution systems. I. A new formulation and the overall problem," *IEEE Trans. Power Del.*, vol. 5, no. 2, pp. 634–642, Apr. 1990.

[17] G. Harrison and A. Wallace, "Optimal power flow evaluation of distribution network capacity for the connection of distributed generation," *Proc. Inst. Elect. Eng., Gener., Transm., Distrib.*, vol. 152, no. 1, pp. 115–122, 2005.

[18] L. Ochoa and G. Harrison, "Minimizing energy losses: Optimal accommodation and smart operation of renewable distributed generation," *IEEE Trans. Power Syst.*, vol. 26, no. 1, pp. 198–205, Feb. 2011.

[19] D. Thukaram and C. Vyjayanthi, "Relative electrical distance concept for evaluation of network reactive power and loss contributions in a deregulated system," *IET Gener., Transm., Distrib.*, vol. 3, no. 11, pp. 1000–1019, 2009.

[20] R. D. Zimmerman, "Matpower User's Manual," Tech. Rep., Power Systems Engineering Research Center, 2010.

[21] Singapore Electricity Tariffs, Singapore Power Group, Mar. 2013 [Online]. Available: http://bit.ly/1bqZFt1

[22] S. X. Chen and H. B. Gooi, "Jump and shift method for multi-objective optimization," *IEEE Trans. Ind. Electron.*, vol. 58, no. 10, pp. 4538–4548, Oct. 2011.

[23] R. Fourer, D. M. Gay, and B. W. Kernighan, *AMPL : A Modeling Language for Mathematical Programming*. Stamford, CT, USA: Thomson Brooks/Cole, 2003.

[24] Ziena Optimization Experts in Nonlinear Optimization, Z. O. LLC, Apr. 2013 [Online]. Available: http://www.ziena.com/knitro.htm

[25] Installation of Capacitor Bank to Improve the Power Factor, SWCC, 2006 [Online]. Available: http://bit.ly/WIeW5x

[26] Parameters of Capacitor Banks Connection Cables, May 2013 [Online]. Available: http://bit.ly/17Vv5ey

[27] High Load Situation for 59 Buses Distribution Power System, May 2013 [Online]. Available: http://bit.ly/ZX4xUo

[28] Low Load Situation for 59 Buses Distribution Power System, May 2013 [Online]. Available: http://bit.ly/ZX4yYE

[29] Branch Parameters for 59 Buses Distribution Power System, May 2013 [Online]. Available: http://bit.ly/ZX4zM2
[30] A Normal Load Situation for 59 Buses Distribution Power System, May 2013 [Online]. Available: http://bit.ly/ZX4AQ4

**S. X. Chen** (M'13) received the B.S. dual degree in power engineering and business administration from Wuhan University, China, and the M.S. and Ph.D. degrees in power engineering from Nanyang Technological University (NTU), Singapore, in 2007, 2008, and 2012, respectively.

From 2012 to 2013, he was a research fellow of the Energy Research Institute at NTU. Currently he works at DNV GL Energy (formerly KEMA). His research interests are smart energy management systems, energy efficiency, power system operation and planning, renewable energy sources, and energy storage systems.

**Y. S. Foo, Eddy** (S'09) received the B.Eng. degree in electrical and electronic engineering from the Nanyang Technological University, Singapore, in 2009 where he is currently pursuing the Ph.D. degree in the Laboratory for Clean Energy Research, School of Electrical and Electronic Engineering.

His research interests are multi-agent systems, microgrid energy management systems, electricity markets, and renewable energy resources.

**H. B. Gooi** (SM'95) received the B.S. degree from National Taiwan University, the M.S. degree from the University of New Brunswick, and the Ph.D. degree from Ohio State University in 1978, 1980, and 1983, respectively.

From 1983 to 1985, he was an Assistant Professor in the Electrical Engineering Department at Lafayette College, Easton, PA, USA. From 1985 to 1991, he was a Senior Engineer with Empros (now Siemens), Minneapolis, MN, USA where he was responsible for the design and testing coordination of domestic and international energy management system (EMS) projects. In 1991, he joined the School of Electrical and Electronic Engineering, Nanyang Technological University, Singapore, as a Senior Lecturer. Since 1999, he has been an Associate Professor. Since 2008, he has served as Deputy Head of Power Engineering Division. His current research focuses on microgrid energy management systems, electricity markets, spinning reserve, energy efficiency and renewable energy sources.

**M. Q. Wang** (M'11) received the Ph.D. degree from Nanyang Technological University (NTU), Singapore, in 2012.

From 2012 to 2013, he was a research fellow of the Energy Research Institute at NTU. Since 2013, he has been a lecturer of the School of Electrical Engineering, Shandong University, Jinan, China. His research interests are power system economic operation and microgrids.

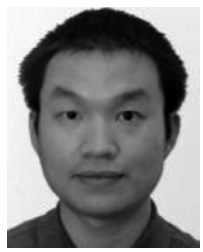

**S. F. Lu** received the B.Eng. and Ph.D. degrees from the University of Birmingham, U.K., in 2007 and 2011, respectively, both in electrical and electronic engineering.

He has been a lecturer with the Department of Electrical and Electronic Engineering, Xi'an Jiaotong-Liverpool University, Xi'an, China, since 2013. From 2011 to 2012, he was a facility manager/research fellow at the University of Birmingham and from 2012 to 2013, he was a research fellow of the Energy Research Institute at Nanyang Technological University, Singapore. His main research interests include power management strategies, railway traction system modelling, and optimization techniques applications.